ORIGINAL ARTICLE

Eur. J. Anat. 24 (6): 491-499(2020)

The architecture of the 6-month-old gastrocnemius: a 3D volumetric study

Luke R. Bradshaw[1], Ethan M. Breinhorst[1], Ngaire S. Stott[2], Anne M.R. Agur[3], Seyed A. Mirjalili[1]

[1]Department of Anatomy and Medical Imaging, University of Auckland, Auckland, New Zealand
[2]Department of Surgery, School of Medicine, University of Auckland, Auckland, New Zealand
[3]Division of Anatomy, Department of Surgery, Faculty of Medicine, University of Toronto, Toronto, Canada

SUMMARY

Gastrocnemius is essential in normal gait, contributing to the control of ankle plantarflexion and knee flexion. However, there is a paucity of literature on the architecture of the infant gastrocnemius muscle prior to the onset of weight-bearing and gait. This study investigates the three-dimensional (3D) musculoaponeurotic architecture of the gastrocnemius in a six-month-old infant. One six-month-old cadaver was used in this study (The University of Toronto Health Sciences Research Ethics Board, #32679, and The University of Auckland Human Participants Ethics Committee, #016164). Medial (MG) and lateral (LG) heads of the gastrocnemius were serially dissected and a Microscribe G2X™ digitizer used to digitize fiber bundles, aponeuroses and tendons. Data were then exported to Autodesk® Maya® to create 3D models. Custom software quantified architectural parameters, including fiber bundle length, pennation angle, physiological cross-sectional area, and muscle volume. The intramuscular architecture was assessed to determine whether musculoaponeurotic partitions were present. Muscle volume was <1cm3 for both MG and LG. Three architectural partitions, proximal, middle, and distal, were identified for both MG and LG. Notably, the proximal partitions of both MG and LG had mean fiber bundle length at 2.21 ± 0.41 cm and 2.22 ± 0.27 cm, significantly greater ($p<0.05$) than the middle and the distal partitions. The results of this study suggest that both MG and LG have architectural partitions before the commencement of gait. Further longitudinal studies with larger sample sizes are needed to confirm the presence of these architectural partitions, as well as to investigate their growth across the developmental spectrum.

Key words: Gastrocnemius – Infant – Muscle architecture – Skeletal muscle – Digitization – Growth – Development

INTRODUCTION

The gastrocnemius muscle is described as a pennate muscle with two heads, medial (MG) and lateral (LG), with each receiving motor branches

Corresponding author: Luke Rafael Bradshaw. The University of Auckland, Department of Anatomy and Medical Imaging, 85 Park Road, Grafton, 1023 Auckland, New Zealand. .
E-mail: lbra285@aucklanduni.ac.nz

Dissemination history.
-Oral presentation at the Australian and New Zealand Association of Clinical Anatomists, Townsville, Australia, held from 2-5th December, 2018.
-Oral presentation at the 2nd World Congress on Undergraduate Research, Oldenburg, Germany, held from 23 – 25th May, 2019

Submitted: 15 May, 2020. *Accepted:* 26 July, 2020.

independently from the tibial nerve. The patterns of intramuscular innervation of both heads of the gastrocnemius have been found to be similar, and identify three neuromuscular partitions; superior, inferomedial and inferolateral, each with its own intramuscular innervation (Robinson et al., 2016). The two heads originate proximally from the medial and lateral femoral condyles and, together with the soleus muscle, make up the triceps surae, which inserts distally to the calcaneus via the calcaneal tendon. The triceps surae is a major power generator in gait and acts to plantarflex the ankle during the terminal stance phase of the gait cycle (Perry, 1992).

While contributing to plantar flexor power generation and knee flexion control, MG and LG differ functionally, both in quiet standing and during active movements. Héroux et al. (2014) reported that, in quiet standing, stability to the ankle is provided by continuous activity of the soleus to counteract static gravitational torque, while MG is only intermittently active in response to anterior-posterior and medio-lateral torque (Héroux et al., 2014). In contrast, LG is inactive in quiet standing and only fires when there is an anterior trunk lean similar to that seen in a stepping response. To explain this finding, Héroux et al. (2014) propose that the two heads of the gastrocnemius work in different ankle ranges, with the fascicle orientation of MG advantaging it in a standing position. Functional differences are also seen during active toe rise tests, with greater activity in MG and sub-volume differences, with greater activation in the proximal part of the muscle (Segal and Song, 2005).

These reported functional differences between MG and LG have been related to differences in the gross morphology and architecture of the two heads. In the adult, MG has a consistently larger muscle volume (MV) than LG (Fukunaga et al., 1992), and extends further distally in most cases (Antonios and Adds, 2008). The fiber bundle (FBs) in MG also have a greater pennation angle (PA) and shorter mean fiber bundle length (FBL) consistent with greater force-generating capabilities as estimated by the physiological cross-sectional area (PCSA), which is the sum of the cross-sectional areas of a muscle's FBs, taking into account their PA. The lateral head, with its smaller MV, longer FBL and smaller PA, would be expected to have less force-generating capability and greater excursion capabilities (Fukunaga et al., 1992).

In contrast to the adult literature, the morphology and intramuscular architecture of MG and LG have not been elucidated in the pediatric population. We could not find any cadaveric studies describing the contractile and connective tissue elements of pediatric gastrocnemius. A limited number of imaging studies were identified. However, only select architectural parameters were quantified from a small number of FBs, often from unknown locations within the muscle volume (Table 1). Typically, the age range of participants in the imaging studies was large, and the data was analyzed as one group. This made it difficult to discern how muscle architecture changes during growth. Notably, from birth to two years of age, there was a paucity of studies. This knowledge gap in normal musculoskeletal development is substantial, impeding understanding of early disease processes that interfere with normal infant musculoskeletal development. Thus, the aim of this paper is to investigate the three-dimensional (3D) musculoaponeurotic architecture of the gastrocnemius in a six-month-old infant, using digitization, 3D modeling and parameter quantification.

MATERIALS AND METHODS

One formalin embalmed six-month-old female infant with no known musculoskeletal abnormalities was included in this study. Ethics approval was received from the University of Toronto Health Sciences Research Ethics Board (Protocol Reference #32679) and the University of Auckland Human Participants Ethics Committee (Protocol Reference #016164).

Entire body computed tomography (CT) scans of the infant were obtained using an Aquilion ONETM Computed Tomography scanner (Toshiba Medical Systems Corporation, Tokyo, Japan). Following scanning, the skin and superficial fascia were excised to expose the underlying deep fascia, which was then removed to expose the superficial surface of MG, LG, and the calcaneal tendon to its insertion.

Fiber bundles on the superficial surface of MG and LG were meticulously delineated from their proximal to their distal attachment sites and digitized at 3-5 mm intervals using a MicroScribeTM G2X Digitizer (0.05 mm accuracy; Immersion Corporation, San Jose, CA). Once the FBs were digitized, they were removed to expose the underlying FBs. This process was repeated until the entire muscle volume had been digitized. During digitization, when aponeuroses, tendons or septa were revealed, the surface of each was digitized using a grid pattern. The digitized data were used to create the 3D muscle models in Autodesk® Maya® with additional software developed in the laboratory.

Muscle belly length was computed using the 3D muscle models and the distance measure tool.

The 3D models were then used to document the spatial arrangements of the FBs and their attachment sites to aponeuroses and tendons. Next, mean FBL, mean PA, PCSA and MV, were quantified from the digitized data using software developed in the laboratory (Lee et al., 2012; 2015). The arrangement of the contractile and connective tissue elements and the quantified architectural parameters were compared between MG and LG. The intramuscular architecture of each head was assessed, using the 3D models and the architec-

Table 1. Imaging studies quantifying pediatric medial gastrocnemius and lateral gastrocnemius architectural parameters in typically developing participants.

Study	Imaging	Mean age, years ± 1SD (range)	Muscle	Mean Architectural Parameters (± 1SD)			
				FBL (cm)	PA (°)	PCSA (cm^2)	MV (cm^3)
Barber et al. (2011b)	US	4.0± 1.2	MEDIAL GASTROCNEMIUS	X	X	7.3± 0.5	33± 2
Barber et al. (2016)	US	5.3± 1.3 (2.3-8.9)	MEDIAL GASTROCNEMIUS	X	X	X	47.8± 17.9
Herskind et al. (2016)	US, MRI	4.0	MEDIAL GASTROCNEMIUS	X	X	X	40*
Kawano et al. (2018)	US	6.4± 1.3	MEDIAL GASTROCNEMIUS	3.14 ±0.32	25.9± 3.2	X	X
Kruse et al. (2018)	US	11.5± 2.5	MEDIAL GASTROCNEMIUS	4.4± 0.8	18.1± 2.7	X	X
Legerlotz et al. (2010)	US	6.6± 2.3 (4-10)	MEDIAL GASTROCNEMIUS	4.12± 0.62	15.7± 1.8	X	X
Malaiya et al. (2007)	US	9.5 (4-13)	MEDIAL GASTROCNEMIUS	4.5± 0.7	17.0± 1.9	X	82.1± 27.3
Obst et al. (2017)	US	4.6± 2.0	MEDIAL GASTROCNEMIUS	X	X	X	46.8± 23.7
Schless et al. (2018)	US	8.2± 1.4	MEDIAL GASTROCNEMIUS	X	X	X	53.6± 12.2
Schless et al. (2019a)	US	9.9± 2.4	MEDIAL GASTROCNEMIUS	X	X	X	68.1± 20.6
Schless et al. (2019b)	US	9.9 (7.8 – 11.5)	MEDIAL GASTROCNEMIUS	X	X	X	62.0
Shortland et al. (2002)	US	7.8 (7-11)	MEDIAL GASTROCNEMIUS	3.74± 1.01	21.7± 4.6	X	X
Willerslev-Olsen et al. (2018)	US	1.4± 1.1	MEDIAL GASTROCNEMIUS	X	X	X	14.1± 9.1
Wren et al. (2010)	US	8.8± 2.3	MEDIAL GASTROCNEMIUS	X	17.9± 2.5	X	X
Mohagheghi et al. (2008)	US	9.1±2.3 (4-14)	MEDIAL GASTROCNEMIUS	4.2± 0.5	X	X	X
			LATERAL GASTROCNEMIUS	4.9± 0.6	X	X	X
Morse et al. (2008)	US, MRI	10.9±0.3	LATERAL GASTROCNEMIUS	7.01± 0.79	10.8± 2.5	15.5± 3.2	64.5± 18.9
Stephensen et al. (2012)	US	9.86± 1.30	LATERAL GASTROCNEMIUS	5.63± 1.02	15.83± 4.21	X	X
Chen et al. (2018)	US	4.83± 1.98	MEDIAL GASTROCNEMIUS	3.70± 0.48	15.4±3.3	X	X
			LATERAL GASTROCNEMIUS	4.51± 0.72	10.7±2.0	X	X

FBL, fiber bundle length; LATERAL GASTROCNEMIUS, lateral head of gastrocnemius; MEDIAL GASTROCNEMIUS, medial head of gastrocnemius; MRI, magnetic resonance imaging; MV, muscle volume; PA, pennation angle; SD, standard deviation; US, ultrasound; X, not reported; *MV was calculated from regression line at 4 years.

tural data, to determine whether MG and LG had musculoaponeurotic partitions. Partitioning was based on the orientation and attachment sites of FBs to aponeuroses and tendons, and the differences in architectural parameter data of FBs in each partition. Statistically significant differences

Table 2. The architectural parameters and attachment sites of medial and lateral gastrocnemius and their architectural partitions

Partition	Proximal attachment	Distal attachment	Mean FBL (mm)	Mean proximal PA (°)	Mean distal PA (°)	PCSA (cm^2)	MV (cm^3)
MED. GSTRC.	Posteromedial cartilaginous distal femoral epiphysis via a flat tendon	Common aponeurosis contributing to the calcaneal tendon distally	19.8±3.2	12.2±5.5	17.1±6.2	0.39	0.80
Proximal (Fig. 2A – D)	Medial aspect of the distal femoral epiphysis, and the superior third of the anterior surface of the superficial aponeurosis	Posterior surface of the medial deep aponeurosis	21.2±4.1[a]	16.9±5.1[c]	21.0±4.0[f]	0.07	0.16
Middle (Fig. 2A – C)	Middle third of the anterior surface of the superficial aponeurosis	Proximal half of the posteromedial surface of the common aponeurosis	19.3±2.0[b]	8.80±4.0[d]	18.0±6.6[g]	0.14	0.28
Distal (Fig. 2A – B)	Inferior third of anterior surface of the superficial aponeurosis	Inferior half of the posteromedial surface of the common aponeurosis	19.1±3.2[b]	13.4±4.6[e]	13.2±4.8[h]	0.16	0.32
LAT. GSTRC.	Posterolateral cartilaginous distal femoral epiphysis via a flat tendon	Common aponeurosis contributing to the calcaneal tendon distally	19.3±3.7	17.0 ± 6.3	10.4±5.3	0.40	0.83
Proximal (Fig. 3A – D)	Inferior half of the anterior surface of the proximal tendon	Lateral edge of the medial deep aponeurosis	22.2±2.7[i]	16.0±5.8[l]	9.97±4.5[n]	0.14	0.32
Middle (Fig. 3A – C.)	Superior three quarters of the anterior surface of the superficial aponeurosis	Posterior surface of the lateral deep aponeurosis and proximal third of the posterolateral surface of the common aponeurosis	17.6±2.5[j]	16.2±5.8[l]	9.25±5.9[n]	0.15	0.30
Distal (Fig. 3A – B)	Distal quarter of the anterior surface and margins of the superficial aponeurosis	Middle third of the posterolateral surface of the common aponeurosis	15.1±1.5[k]	21.5±6.8[m]	13.7±5.1[o]	0.07	0.12

between architectural parameters of MG and LG were tested using student t- tests, and between partitions using one-way ANOVA, with significance set at $p<0.05$. These statistical analyses were performed using SSPS statistical software Version 25 (IBM Corp., Armonk, N.Y., USA).

RESULTS

The 3D models provide insight into the in-situ attachment sites and morphology of the medial and lateral heads (Fig. 1). Proximally, both heads attached to the cartilaginous distal femoral epiphysis via a flat tendon, MG to the posteromedial surface of the epiphysis, and LG to the posterolateral surface. Distally, each tendon expanded to form a superficial aponeurosis spanning the proximal two-thirds of the medial and lateral muscle bellies. The muscle belly of the medial head, at 5.34 cm in length, extended further distally than that of the lateral head, with a length of 4.84 cm. Both MG and LG had a second, deep aponeurosis located on the anterior surface of their muscle belly. The deep aponeuroses of each head converged to form a common aponeurosis, which, together with a contribution from soleus, formed the calcaneal tendon (Fig. 1A, iv). The calcaneal tendon could be traced to its distal attachment on the posterior aspect of the cartilaginous calcaneus.

Both MG and LG were found to consist of three overlapping partitions arranged from superficial to deep (Figs. 1B, 1C). In each head, the distal partition was most superficial, followed by the middle and proximal partitions. These partitions were defined on the basis of morphology, attachment sites, PA, and FBL.

All of the partitions of MG and LG attached superiorly to specific regions on either the medial and lateral femoral epiphysis and/or the anterior surface of the superficial aponeurosis. Inferiorly, the partitions attached to well-defined areas of the deep and common aponeuroses. Table 2 outlines the specific partition attachment sites.

The mean FBL of MG and LG were similar (Table 2). However, at the partition level, the proximal partition of each head had the greatest mean FBL. The middle partition of LG had significantly greater mean FBL than the distal partition ($p<0.05$); in MG, no significant difference was found.

Significant differences in mean PA were observed between MG and LG, with the mean proxi-

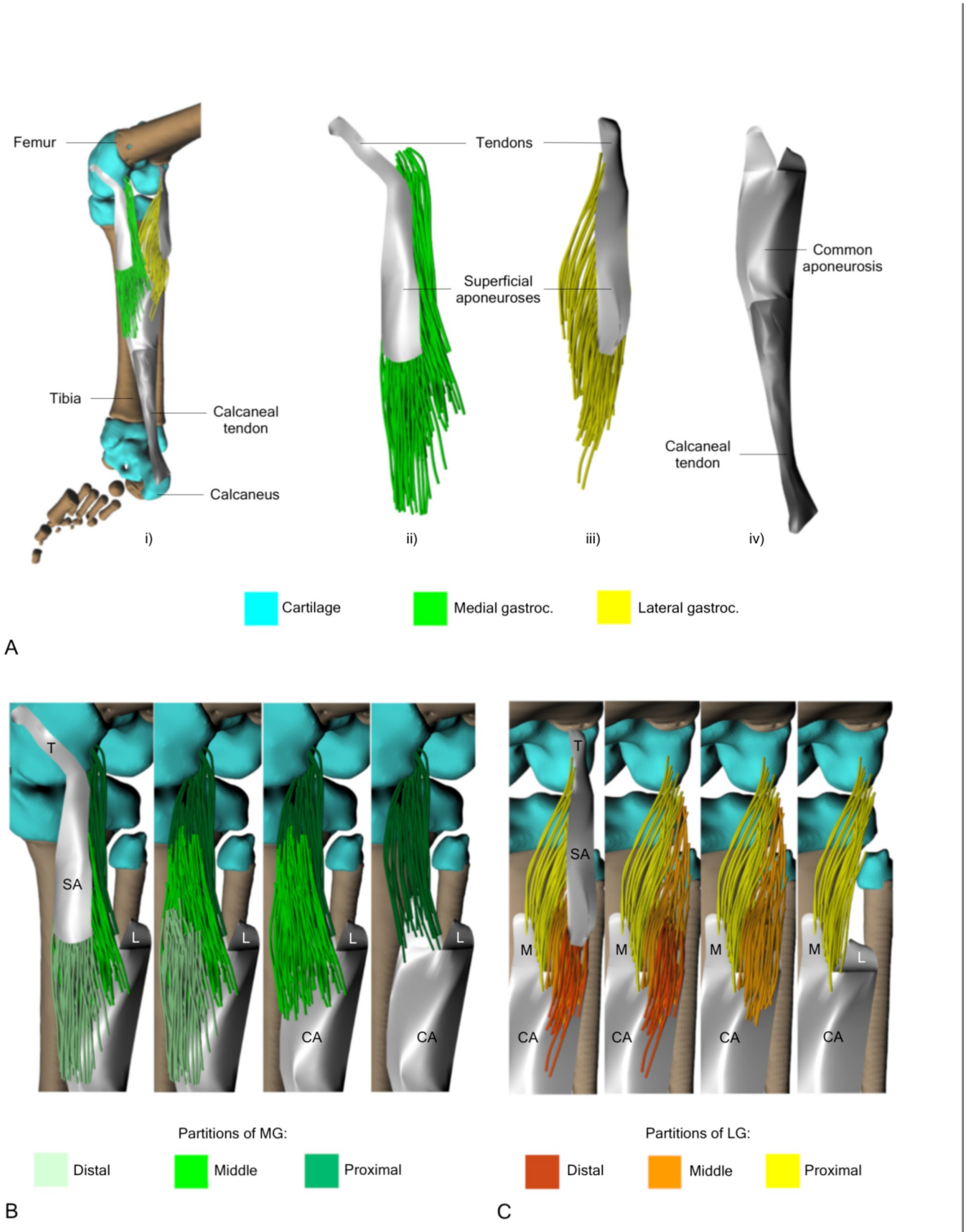

Fig 1. A. i) MG and LG registered to the 3D surface reconstruction of infant skeleton. ii) Medial head of gastrocnemius. iii) Lateral head of gastrocnemius. iv) Connective tissue elements deep to MG and LG muscle bellies, and the calcaneal tendon. **B.** Partitions of MG. **C.** Partitions of LG. CA, common aponeurosis; L, deep aponeurosis of LG; LG, lateral head of gastrocnemius; M, deep aponeurosis of MG; MG, medial head of gastrocnemius; SA, superficial aponeurosis.

mal PA of MG being 4.8° less than the LG ($p<0.05$), and its mean distal PA 6.7° greater ($p<0.05$) (Table 2). In LG, the greatest mean proximal and distal PA were found in the distal partition, while no significant difference in mean PA was found between the proximal and middle partitions. In MG, although the mean distal PA decreased from proximal to distal, this pattern was not evident for mean proximal PA. Notably, both the proximal partition in MG and the distal partition in LG had the greatest mean proximal and distal

PA within their respective heads.

The PCSA and MV of MG and LG were similar. However, the distribution of PCSA and MV at the partition level differed between each head. The proximal partition of MG had approximately half the MV and half the PCSA of the middle and distal partitions. In LG, this pattern was reversed, with the distal partition having half the MV and PCSA of the middle and proximal partitions.

DISCUSSION

This is the first study to quantify the 3D musculoaponeurotic architecture of MG and LG in a six-month-old infant. The morphological arrangement of the contractile and connective tissue elements and their attachment sites were similar in the six-month-old and the adult; however, the architectural parameters differed significantly.

Musculoaponeurotic morphology

In the adult, the muscle belly length of MG is typically greater than LG; the difference in mean muscle belly length has been reported in four studies and ranged from 2-15% (Wickiewicz et al., 1983; Friederich and Brand, 1990; Fukunaga et al., 1992; Morse et al., 2005a). In the current study, a similar finding was noted, with the muscle belly length of the MG being 10% greater than LG. Consistent with the adult, FBs of MG and LG in the infant had three partitions (Robinson et al., 2016). This suggests that both MG and LG may have neuromuscular partitions in the six-month-old infant, before the commencement of gait. However, further study is needed to determine intramuscular innervation patterns in the infant.

In adult literature and the current study, MG and LG had flat proximal tendons, extending distally from their proximal attachment to form superficial aponeuroses, covering the superficial two-thirds of each muscle belly. The anterior surface of these aponeuroses provided attachment for FBs on their anterior surface (Dalmau-Pastor et al., 2014).

In the current study, and in the adult, FBs of each head travelled inferiorly to converge with those of the opposite head before attaching to the posterior surface of separate aponeuroses. These joined to form a single wide aponeurosis, which contributed to the formation of the calcaneal tendon (Dalmau-Pastor et al., 2014).

In the adult, the proximal fiber bundles of MG and LG have been reported to attach to the medial and lateral supracondylar ridges, superior to the tendinous attachment on the medial and lateral femoral condyles, respectively (Dalmau-Pastor et al., 2014). In the infant MG, this attachment was conserved; however in LG, fiber bundle attachment to the femur was not present.

Architectural parameters

The results of the current study were compared to pediatric and adult literature. Typically, the age range of participants in the pediatric literature was large, and architectural data reported as a mean for the entire participant group, making it difficult to discern developmental trends. In the current study, the total MV of both MG and LG was less than 1 cm3. The MV of pediatric MG was recorded in seven studies, ranging from 14.1 cm3 at a mean age of 1.4 years to 82.1 cm3 at a mean age of 9.5 years (Malaiya et al., 2007; Barber et al., 2011b; Herskind et al., 2016; Barber et al., 2016; Obst et al., 2017; Schless et al., 2018; Willerslev-Olsen et al., 2018; Schless et al., 2019a, 2019b). All except one of the adult studies reported a mean MV greater than 200 cm3 (Fukunaga et al., 1992; Narici et al., 1996; Elliott et al., 1997; Narici et al., 2003; Albracht et al., 2008; Csapo et al., 2010; Tomlinson et al., 2014; Hussain et al., 2017; Morse et al., 2015). Pediatric LG was reported to have an MV of 64.5 cm3 at 10.9 years by Morse et al. (2008); all adult studies reported MV greater than 140 cm3 (Fukunaga et al., 1992; Elliott et al., 1997; Morse et al., 2005b; Albracht et al., 2008).

These data suggest that MG and LG increase in volume at least 100-fold across the developmental spectrum from infancy to adulthood. A lack of literature makes it difficult to comment on age-specific growth rates, but these data suggest that a tenfold increase may occur within the first two years of life. However, the comparison between the MV of each head at different stages of development suggests disproportionate growth. In the current study, there is less than a 4% difference between the MV of MG and LG. However, literature investigating the MV of both MG and LG in adult participants suggests that this similarity is not present upon maturation of gastrocnemius architecture, with all studies reporting that the mean MV of MG was at least twice that of LG (Fukunaga et al., 1992; Elliott et al., 1997; Albracht et al., 2008).

A review of the published literature showed that the mean FBL of LG compared to MG was longer in all pediatric and adult studies. Pediatric MG, in six ultrasound studies, was reported to have a mean FBL ranging from 3.1 cm to 4.5 cm with mean participant ages of 4.8 to 11.5 years (Shortland et al., 2002; Malaiya et al., 2007; Mohagheghi et al., 2008; Legerlotz et al., 2010; Chen et al., 2018; Kruse et al., 2018; Kawano et al., 2018). For pediatric LG, mean FBL of 4.9 cm to 7.0 cm were recorded in four ultrasound studies with mean participant ages from 4.8 to 10.9 years (Mohagheghi et al., 2008; Morse et al., 2008; Stephensen et al., 2012; Chen et al., 2018).

Comparison of the architectural parameters of the six-month-old infant in the current study and the pediatric study with the youngest mean age (4.8 years), by Chen et al. (2018), suggests an 87% (1.7 cm) increase in the mean FBL of MG, and a 134% (2.6 cm) increase in the mean FBL of LG from six months to 4.8 years. In contrast, com-

parison between Chen et al. (2018) and the adult (Agur et al. 2003) revealed a 21% (0.78 cm) increase in mean FBL for MG and a 28% (1.27 cm) increase for LG. This suggests that the majority of the increase in mean FBL between the infant and the adult occurs during the first few years of development. However, the comparison between each head suggests a disproportionately greater increase in mean FBL for LG across the developmental timeline.

The mean distal PA of MG and LG in the current study were similar to those reported in the pediatric literature; no record of the mean proximal PA was found. For MG, the mean distal PA ranged from 15.4° - 25.9° in six ultrasound studies, with mean participant ages of 4.8 to 11.5 years (Shortland et al., 2002; Malaiya et al., 2007; Legerlotz et al., 2010; Wren et al., 2010; Chen et al., 2018; Kruse et al., 2018; Kawano et al., 2018). In three studies that recorded the mean distal PA of LG, it was found to range from 10.7° - 15.8° (mean participant age of 4.8 - 10.9 years). The mean distal PA of MG and LG in the current study were similar to the pediatric literature. However, in the adult, the mean distal PA of MG and LG decreased by 8.2° and 3.9°, respectively, when compared to the pediatric literature (Agur et al., 2003). This suggests that a large proportion of change in distal PA occurs later in development.

Literature quantifying the PCSA of pediatric MG and LG was scarce. Only two studies were found, one investigating MG and the other LG. The PCSA of MG in the current study was 0.39 cm2, increasing to 7.3 cm2 at 4.0 years (Barber et al., 2011b), and at least 41 cm2 in the adult literature (Fukunaga et al., 1992; Narici et al., 1996; Narici et al., 2003; Albracht et al., 2008; Barber et al., 2011a; Csapo et al., 2010; Tomlinson et al., 2014; Morse et al., 2015; Hussain et al., 2017). Similarly, the PCSA of LG increased from 0.40 cm2 in the current study to 15.5 cm2 at 10.9 years, and to a minimum of 24 cm2 in the adult (Fukunaga et al., 1992; Morse et al., 2005b; Albracht et al., 2008). This suggests that there are large increases in the PCSA of MG and LG throughout the developmental spectrum. Interestingly, this increase was not proportionate. In the current study, the PCSA of MG and LG were similar. However, by adulthood the mean PCSA of MG was approximately two to three times greater than LG (Fukunaga et al., 1992; Albracht et al., 2008).

Limitations

The main limitation of this study is the sample size of one. This reflects a scarcity of infant donations to research programs due to regional laws and regulations. It was therefore not possible to conduct a longitudinal study; comparison had to be made directly with the adult, with little intermediate data to guide analysis. A sample size of one also meant that the degree of architectural variation within the infant population, including sexual variation, could not be assessed.

Furthermore, as this was a cadaveric study, the tissue properties will differ from in-vivo muscle. This limitation is inherent in all cadaveric studies. However, some studies have documented the relationship of cadaveric to in-vivo muscle tissue properties. Martin et al. (2001) reported that the mean FBL of cadaveric muscle is approximately halfway between relaxed and contracted in-vivo muscle. In another study, Cutts and Seedhom (1993) found that absolute in-vivo muscle parameters were larger than cadaveric measurements. However, this study also reported that the relative PCSAs of in-vivo CT imaged quadriceps muscles were similar to the relative PCSAs calculated from cadaveric data. In the current study, it was only possible to compare cadaveric infant data to in-vivo ultrasound studies as no other infant cadaveric studies were found. The data from the current study will be used to inform novel in-vivo ultrasound protocols to investigate the development of pediatric gastrocnemius.

Functional Implications

Differing functional demands following commencement of weight-bearing activities may play a role in the architectural development of each head, and ultimately the achievement of their respective functions in the adult. In the current study, at six months, similar PCSA and mean FBL of MG and LG suggests that prior to weight- bearing and gait, this divergent functionality is absent. Variations between infant, pediatric, and adult studies suggest a non-linear developmental timeline for the intramuscular architecture of MG and LG. However, due to the scarcity of pediatric literature, a series of longitudinal studies with smaller age ranges are required to elucidate the timing of specific changes in the architectural parameters of each head.

In conclusion, this is the first study to volumetrically quantify the morphology and architectural parameters of gastrocnemius at six months. In both the infant and adult, proximal, middle, and distal partitions were found to be present; however, their architectural parameters differed. The lack of pediatric gastrocnemius muscle architecture studies makes it difficult to comment on the architectural development of the gastrocnemius muscle through childhood. A further longitudinal study of the muscular partitions of the gastrocnemius is required to determine how the muscle architecture changes during development in order to gain an understanding of the architectural basis for the achievement of functional milestones.

ACKNOWLEDGEMENTS

We thank the individuals who donated their bodies and tissue for the advancement of education

and research. We would like to acknowledge J. Tran, M. Stiver, and A. Duong (University of Toronto, Toronto, Canada) for their methodological insights. L.R.B. and E.M.B. thank the University of Auckland for the University of Auckland Postgraduate Honours/P.G. Diploma Scholarship, as well as the University of Auckland School of Medicine Foundation for its support.

REFERENCES

AGUR A, TUBIANI G, LOH E, BABIK D, MCKEE NH (2003) Muscle architecture and innervation patterns of the medial and lateral heads of gastrocnemius: A 3D modelling study. Clin Anat, 16: 542-564.

ALBRACHT K, ARAMPATZIS A, BALTZOPOULOS V (2008) Assessment of muscle volume and physiological cross-sectional area of the human triceps surae muscle in vivo. J Biomech, 41: 2211-2218.

ANTONIOS T, ADDS PJ (2008) The medial and lateral bellies of gastrocnemius: a cadaveric and ultrasound investigation. Clin Anat, 21: 66-74.

BARBER L, BARRETT R, LICHTWARK G (2011a) Passive muscle mechanical properties of the medial gastrocnemius in young adults with spastic cerebral palsy. J Biomech, 44: 2496-2500.

BARBER L, HASTINGS-ISON T, BAKER R, BARRET R, LICHTWARK G (2011b) Medial gastrocnemius muscle volume and fascicle length in children aged 2 to 5 years with cerebral palsy. Dev Med Child Neurol, 53: 543-548.

BARBER LA, READ F, STERN JL, LICHTWARK G, BOYD RN (2016) Medial gastrocnemius muscle volume in ambulant children with unilateral and bilateral cerebral palsy aged 2 to 9 years. Dev Med Child Neurol, 58: 1146-1152.

CHEN Y, HE L, XU K, LI J, GUAN B, TANG H (2018) Comparison of calf muscle architecture between Asian children with spastic cerebral palsy and typically developing peers. PLoS One, 13: e0190642.

CSAPO R, MAGANARIS CN, SEYNNES OR, NARICI MV (2010) On muscle, tendon and high heels. J Exp Biol, 213: 2582-2588.

CUTTS A, SEEDHOM BB (1993) Validity of cadaveric data for muscle physiological cross-sectional area ratios: a comparative study of cadaveric and in-vivo data in human thigh muscles. Clin Biomech, 8: 156-162.

DALMAU-PASTOR M, FARGUES-POLO B, CASANOVA-MARTÍNEZ D, VEGA J (2014) Anatomy of the triceps surae: a pictorial essay. Foot Ankle Clin, 19: 603-635.

ELLIOTT MA, WALTER GA, GULISH H, SADI AS, LAWSON DD, JAFFE W, INSKO EK, LEIGH JS, VANDENBORNE K (1997) Volumetric measurement of human calf muscle from magnetic resonance imaging. Magn Reson Mater Phy, 5: 93-98.

FRIEDERICH JA, BRAND RA (1990) Muscle fiber architecture in the human lower limb. J Biomech, 23: 91-95.

FUKUNAGA T, ROY RR, SHELLOCK FG, HODGSON JA, DAY MK, LEE PL, KWONG-FU H, EDGERTON VR (1992) Physiological cross-sectional area of human leg muscles based on magnetic resonance imaging. J Orthop Res, 10: 926-934.

HÉROUX ME, DAKIN CJ, LUU BL, INGLIS JT, BLOUIN JS (2014) Absence of lateral gastrocnemius activity and differential motor unit behavior in soleus and medial gastrocnemius during standing balance. J Appl Physiol, 116: 140-148.

HERSKIND A, RITTERBAND-ROSENBAUM A, WILLERSLEV-OLSEN M, LORENTZEN J, HANSON L, LICHTWARK G, NIELSEN JB (2016) Muscle growth is reduced in 15-month-old children with cerebral palsy. Dev Med Child Neurol, 58: 485-491.

HUSSAIN AW, ONAMBÉLÉ GL, WILLIAMS AG, MORSE CI (2017) Medial gastrocnemius specific force of adult men with spastic cerebral palsy. Muscle Nerve, 56: 298-306.

KAWANO A, YANAGIZONO T, KADOUCHI I, UMEZAKI T, CHOSA E (2018) Ultrasonographic evaluation of changes in the muscle architecture of the gastrocnemius with botulinum toxin treatment for lower extremity spasticity in children with cerebral palsy. J Orthop Sci, 23: 389-393.

KRUSE A, SCHRANZ C, TILP M, SVEHLIK M (2018) Muscle and tendon morphology alterations in children and adolescents with mild forms of spastic cerebral palsy. BMC Pediatr, 18: 156.

LEE D, LI Z, SOHAIL QZ, JACKSON K, FIUME E, AGUR A (2015) A three-dimensional approach to pennation angle estimation for human skeletal muscle. Comput Methods Biomech Engin, 18: 1474-1484.

LEE D, RAVICHANDIRAN K, JACKSON K, FIUME E, AGUR A (2012) Robust estimation of physiological cross-sectional area and geometric reconstruction for human skeletal muscle. J Biomech, 45: 1507-1513.

LEGERLOTZ K, SMITH HK, HING WA (2010) Variation and reliability of ultrasonographic quantification of the architecture of the medial gastrocnemius muscle in young children. Clin Physiol Funct I, 30: 198-205.

MALAIYA R, MCNEE AE, FRY NR, EVE LC, GOUGH M, SHORTLAND AP (2007) The morphology of the medial gastrocnemius in typically developing children and children with spastic hemiplegic cerebral palsy. J Electromyogr Kines, 17: 657-663.

MARTIN DC, MEDRI MK, CHOW RS, OXORN V, LEEKAM RN, AGUR AM, MCKEE NH (2001) Comparing human skeletal muscle architectural parameters of cadavers with in vivo ultrasonographic measurements. J Anat, 199: 429-434.

MOHAGHEGHI AA, KHAN T, MEADOWS TH, GIANNIKAS K, BALTZOPOULOS V, MAGANARIS CN (2008) In vivo gastrocnemius muscle fascicle length in children with and without diplegic cerebral palsy. Dev Med Child Neurol, 50: 44-50.

MORSE CI, SMITH J, DENNY A, TWEEDALE J, SEARLE ND (2015) Gastrocnemius medialis muscle architecture and physiological cross sectional area in adult males with Duchenne muscular dystrophy. J Musculoskel Neuron, 15: 154.

MORSE CI, THOM JM, BIRCH KM, NARICI MV (2005a)

Changes in triceps surae muscle architecture with sarcopenia. Acta Physiol Scand, 183: 291-298.

MORSE CI, THOM JM, REEVES ND, BIRCH KM, NARICI MV (2005b) In vivo physiological cross-sectional area and specific force are reduced in the gastrocnemius of elderly men. J Appl Physiol, 99: 1050-1055.

MORSE CI, TOLFREY K, THOM JM, VASSILOPOULOS V, MAGANARIS CN, NARICI MV (2008) Gastrocnemius muscle specific force in boys and men. J Appl Physiol, 104: 469-474.

NARICI MV, BINZONI T, HILTBRAND E, FASEL J, TERRIER F, CERRETELLI P (1996) In vivo human gastrocnemius architecture with changing joint angle at rest and during graded isometric contraction. J Physiol, 496: 287-297.

NARICI MV, MAGANARIS CN, REEVES ND, CAPODAGLIO P (2003) Effect of aging on human muscle architecture. J Appl Physiol, 95: 2229-2234.

OBST SJ, BOYD R, READ F, BARBER L (2017) Quantitative 3-D ultrasound of the medial gastrocnemius muscle in children with unilateral spastic cerebral palsy. Ultrasound Med Biol, 43: 2814-2823.

PERRY J (1992) Gait Analysis: Normal and Pathological Function. SLACK Incorporated, New Jersey.

ROBINSON TJG, RAVICHANDIRAN K, SATKUNAM LE, MCKEE NH, AGUR AM, LOH E (2016) Neuromuscular partitioning of the gastrocnemius based on intramuscular nerve distribution patterns: implications for injections. Eur J Anat, 20: 65-73.

SCHLESS SH, HANSSEN B, CENNI F, BAR-ON L, AERTBELIËN E, MOLENAERS G, DESLOOVERE K (2018) Estimating medial gastrocnemius muscle volume in children with spastic cerebral palsy: a cross-sectional investigation. Dev Med Child Neurol, 60: 81-87.

SCHLESS SH, CENNI F, BAR-ON L, HANSSEN B, GOUDRIAAN M, PAPAGEORGIOU E, AERTBELIËN E, MOLENAERS G, DESLOOVERE K (2019a) Combining muscle morphology and neuromotor symptoms to explain abnormal gait at the ankle joint level in cerebral palsy. Gait Posture, 68: 531-537.

SCHLESS SH, CENNI F, BAR-ON L, HANSSEN B, KALKMAN B, O'BRIEN T, AERTBELIËN E, VAN CAMPENHOUT A, MOLENAERS G, DESLOOVERE K (2019b) Medial gastrocnemius volume and echointensity after botulinum neurotoxin A interventions in children with spastic cerebral palsy. Dev Med Child Neurol, 61: 783-790.

SEGAL RL, SONG AW (2005) Non-uniform activity of human calf muscles during an exercise task. Arch Phys Med Rehab, 86: 2013-2017.

SHORTLAND AP, HARRIS CA, GOUGH M, ROBINSON RO (2002) Architecture of the medial gastrocnemius in children with spastic diplegia. Dev Med Child Neurol, 44: 158-163.

STEPHENSEN D, DRECHSLER W, SCOTT O (2012) Comparison of muscle strength and in-vivo muscle morphology in young children with haemophilia and those of age-matched peers. Haemophilia, 18: e302-e310.

TOMLINSON DJ, ERSKINE RM, WINWOOD K, MORSE CI, ONAMBÉLÉ GL (2014) The impact of obesity on skeletal muscle architecture in untrained young vs. old women. J Anat, 225: 675-684.

WICKIEWICZ TL, ROY RR, POWELL PL, EDGERTON VR (1983) Muscle architecture of the human lower limb. Clin Orthop Relat R, 179: 275-283.

WILLERSLEV-OLSEN M, LUND MC, LORENTZEN J, BARBER L, KOFOED-HANSEN M, NIELSEN JB (2018) Impaired muscle growth precedes development of increased stiffness of the triceps surae musculotendinous unit in children with cerebral palsy. Dev Med Child Neurol, 60: 672-679.

WREN TAL, CHEATWOOD AP, RETHLEFSEN SA, HARA R, PEREZ FJ, KAY RM (2010) Achilles tendon length and medial gastrocnemius architecture in children with cerebral palsy and equinus gait. J Pediatr Orthoped, 30: 479-484.